JACS
JOURNAL OF THE AMERICAN CHEMICAL SOCIETY

Article

Cobalt/Lewis Acid Catalysis for Hydrocarbofunctionalization of Alkynes via Cooperative C–H Activation

Chang-Sheng Wang, Sabrina Di Monaco, Anh Ngoc Thai, Md. Shafiqur Rahman, Benjamin Piaoxiang Pang, Chen Wang, and Naohiko Yoshikai

J. Am. Chem. Soc., **Just Accepted Manuscript** • DOI: 10.1021/jacs.0c06412 • Publication Date (Web): 23 Jun 2020

Cobalt/Lewis Acid Catalysis for Hydrocarbofunctionalization of Alkynes via Cooperative C–H Activation

Chang-Sheng Wang,[†] Sabrina Di Monaco,[†,§] Anh Ngoc Thai,[†,∥] Md. Shafiqur Rahman,[†] Benjamin Piaoxiang Pang,[†] Chen Wang,*[,†,‡] and Naohiko Yoshikai*[,†]

[†]Division of Chemistry and Biological Chemistry, School of Physical and Mathematical Sciences, Nanyang Technological University, Singapore 637371, Singapore

[‡]Zhejiang Key Laboratory of Alternative Technologies for Fine Chemical Process, Shaoxing University, Shaoxing 312000, P.R. China

ABSTRACT: A catalytic system comprised of a cobalt–diphosphine complex and a Lewis acid (LA) such as $AlMe_3$ has been found to promote hydrocarbofunctionalization reactions of alkynes with Lewis basic and electron-deficient substrates such as formamides, pyridones, pyridines and related azines, imidazo[1,2-*a*]pyridines, and azole derivatives through site-selective C–H activation. Compared with known Ni/LA catalytic systems for analogous transformations, the present catalytic systems not only feature convenient set up using inexpensive and bench-stable precatalyst and ligand such as $Co(acac)_3$ and 1,3-bis(diphenylphosphino)propane (dppp), but also display distinct site-selectivity toward C–H activation of pyridone and pyridine derivatives. In particular, a completely C4-selective alkenylation of pyridine has been achieved for the first time. Meanwhile, the present catalytic system proved to promote exclusively C5-selective alkenylation of imidazo[1,2-*a*]pyridine derivatives. Mechanistic studies including DFT calculations on the Co/Al-catalyzed addition of formamide to alkyne have suggested that the reaction involves cleavage of the carbamoyl C–H bond as the rate-limiting step, which proceeds through a ligand-to-ligand hydrogen transfer (LLHT) mechanism leading to an alkenyl(carbamoyl)cobalt intermediate.

INTRODUCTION

The transition metal-catalyzed addition of an unactivated C–H bond across unsaturated hydrocarbons such as olefins and alkynes represents an atom-economically ideal approach to C–C bond formation.[1] To achieve this type of hydrocarbofunctionalization reactions in a synthetically useful manner, it is crucial that the catalyst can target a specific C–H bond among others in the given substrate. In this respect, directing groups have been extensively used to ensure high efficiency and site-selectivity of the activation of the proximal C–H bond through chelation assistance. Nevertheless, although powerful and reliable, the covalently linked directing groups inevitably limit the reaction scope to specific types of substrates. Therefore the development of hydrocarbofunctionalization reactions that do not rely on chelation assistance represents an important subject.

Besides substrates bearing directing groups, electronically biased substrates have been successfully employed for hydrocarbofunctionalization via site-selective C–H activation. Among notable strategies to achieve such transformations is the cooperation of electron-rich nickel(0) and Lewis acidic main group metals (e.g., Zn, Al, and B) for the C–H activation of innately Lewis basic and electron-deficient substrates (Scheme 1).[2] In 2008, Nakao and Hiyama first demonstrated the concept of Ni/LA cooperative C–H activation by the C2-selective alkenylation of pyridines with alkynes.[3,4] Thus, coordination of the pyridine nitrogen to Lewis acidic $ZnPh_2$ makes the pyridine core more electron-deficient, thereby enhancing its reactivity toward an electron-rich Ni(0)–trialkylphosphine catalyst. Since this seminal report, Nakao and Hiyama have significantly expanded the scope of Ni/LA catalysis to achieve C–H alkenylation and alkylation of Lewis basic substrates such as pyridines,[5,6] imidazoles,[7,8] formamides,[9] pyridones,[10] aryl carbonyl compounds,[11] and aryl sulfones[12] with alkynes and alkenes, respectively, through appropriate modification of the supporting ligand for Ni(0) and choice of the Lewis acid cocatalyst. The concept of the Ni/LA cooperative C–H activation has also been adopted by other research groups to achieve (enantioselective) intramolecular hydrocarbofunctionalization reactions of pyridones,[13] imidazoles,[14,15] and pyridines[16] through development of novel chiral phosphorus- or *N*-heterocyclic carbene ligands.[17]

Scheme 1. Ni^0/Lewis Acid Cooperative C–H Activation

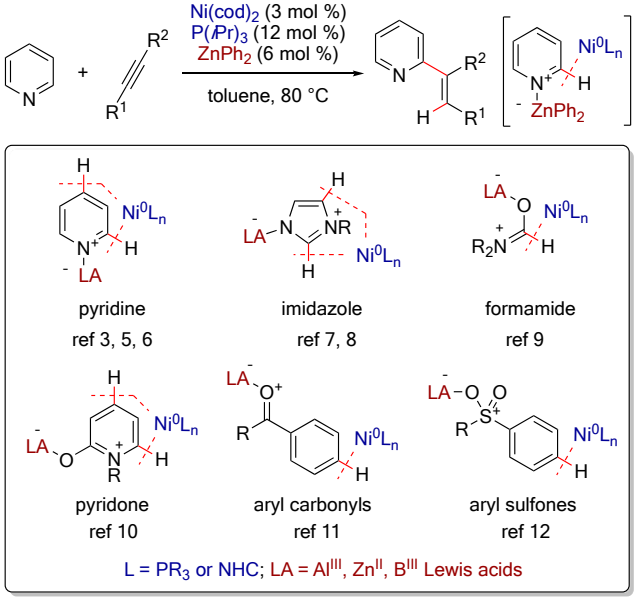

- Other combination of transition metals and Lewis acids?
- Possibility for unique reactivity or site-selectivity?

Given the broad scope and the high tunability of Ni/LA bimetallic catalytic systems, we became interested in the "generality" of the transition metal/Lewis acid cooperative C–H activation. Thus, we wondered if analogous mode of C–H activation is viable with different combinations of low-valent transition metals and Lewis acids. In this respect, our attention was attracted to the parallelism between low-valent nickel and cobalt in the C–H activation of azole derivatives (Scheme 2a). Nakao and Hiyama reported alkenylation of relatively acidic heteroarenes, including benzoxazole, with alkynes promoted by a Ni(0)–trialkylphosphine catalyst.[18,19] Later, we demonstrated alkenylation of (benz)oxazole and (benzo)thiazole derivatives using low-valent Co–diphosphine catalyst generated by reduction of a Co(II) salt with a Grignard reagent,[20,21] which appeared to share a similar mechanistic pathway with the Ni(0) catalysis. Meanwhile, our exploration of low-valent Co–diphosphine catalysts generated from Co(II) and metallic reductant for alkyne transformations[22] led us to come across a notable side reaction, that is, the addition of DMF (used as solvent) to an internal alkyne through carbamoyl C–H bond cleavage.[23] This observation, together with the apparent parallelism between Ni and Co for the benzoxazole C–H activation, inspired us to explore Co/LA catalysis for cooperative C–H activation.[24]

Herein, we report that the combination of cobalt–diphosphine and Lewis acid catalysts is highly effective for hydrocarbofunctionalization of alkynes with Lewis basic and electron-deficient substrates, including formamides, pyridones, pyridines and related azines, imidazo[1,2-*a*]pyridines, and azole derivatives, via site-selective C–H activation (Scheme 2b). Compared with typical Ni/LA catalytic systems comprised of air-sensitive $Ni(cod)_2$ and electron-rich trialkylphosphine or N-heterocyclic carbene, the present systems are easy to set up using air- and moisture-stable precatalyst ($Co(acac)_3$) and diphosphine ligand (dppp), the latter serving as a common inexpensive ligand encompassing diverse classes of substrates. Furthermore, the Co/LA systems have proven to show distinct site selectivity compared with the known Ni/LA systems in the C–H activation of pyridone and pyridine derivatives. Mechanistic studies have suggested that the Co/Al-catalyzed addition of a formamide to an alkyne involves a rate-limiting bimetallic C–H bond cleavage process that occurs through a ligand-to-ligand hydrogen transfer (LLHT) mechanism.[25]

Scheme 2. Parallelism between Ni and Co Catalysis and This Work

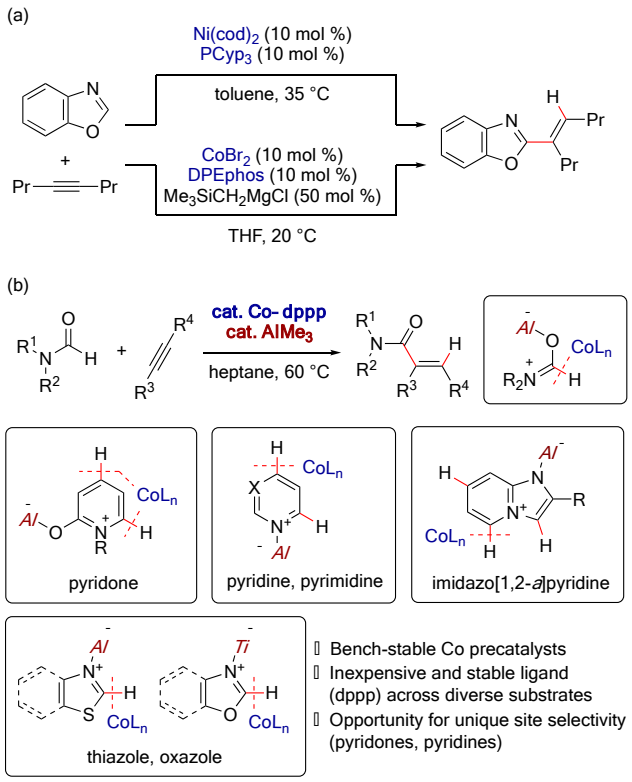

RESULTS AND DISCUSSION

Discovery of Co/Al Cooperatively Catalyzed Hydrocarbamoylation of Alkynes. We have demonstrated that low-valent cobalt catalysts generated from cobalt salts, supporting ligands, and Grignard reagents promote hydroarylation reactions of alkynes and alkenes via chelation-assisted C–H activation.[21a,26] While a catalyst generated by the same reduction method is used, the C2-alkenylation of azole derivatives (Scheme 2a) is distinct from these chelation-assisted hydroarylations. However, the parallelism between this C2-alkenylation and the analogous Ni(0)-catalyzed reaction has long escaped our attention. In the meantime, we have explored another type of low-valent cobalt catalysts, generated from cobalt(II) salt, diphosphine ligand, and metallic reductant (e.g. Zn), for hydroacylation,[27] cycloaddition,[22a,b] and homoenolate transformation.[22d] On studying alkyne cycloaddition using this type of cobalt–diphosphine catalyst,[28,29] we have observed the addition of DMF (solvent) to an internal alkyne to afford an α,β-unsaturated amide as a byproduct. This alkyne hydrocarbamoylation reaction is reminiscent of the one catalyzed by Ni/Al catalyst,[9a,30] and has triggered our interest in the feasibility of C–H activation by Co/LA cooperative catalysis.

Table 1 summarizes results of the addition of DMF (**1a**) to 5-decyne (**2a**) under various Co and Co/LA catalytic systems (see Tables S1–S6 for detailed optimization results). We first found that, in DMF as solvent, a catalyst generated from CoI_2 (2.5 mol %), dppp (2.5 mol %), and Zn (25 mol %) promoted the

hydrocarbamoylation to **2a** to afford the α,β-unsaturated amide **3aa** in good yield of 71% with exclusive *syn*-selectivity (entry 1), which was accompanied by a small amount (5%) of hexabutylbenzene formed by cyclotrimerization of **2a**. The yield of **3aa** could be improved to 99% by the addition of DABCO (25 mol %; entry 2). However, no hydrocarbamoylation took place when the amount of **1a** was reduced to 2 equiv and the reaction was performed with 5 mol % each of CoI_2 and dppp in toluene at 60 °C (entry 3). In stark contrast, the addition of $AlMe_3$ (20 mol %) to this system dramatically promoted the hydrocarbamoylation to afford **3aa** in 99% yield (96% isolated yield; entry 4). Other cobalt precatalysts such as $CoBr_2$, $CoCl_2$, and $Co(acac)_3$ also proved effective, with slightly deviating yields of **3aa** (entries 5–7). Zn could be omitted from the catalytic system, while in such case the catalytic activity was largely dependent on the precatalyst. Thus, a catalytic system comprised of $Co(acac)_3$, dppp, and $AlMe_3$ efficiently promoted the hydrocarbamoylation in heptane (entry 8), while the reaction became rather sluggish using CoI_2 or $CoBr_2$ (Table S3). A preformed Co(I) complex $CoCl(PPh_3)_3$ also served as a viable precatalyst in the absence of Zn (entry 9), while no reaction was observed using $Co_2(CO)_8$ (entry 10).

Diphosphine ligands other than dppp also gave rise to active catalysts, albeit with reduced efficiency (entries 11 and 12), while no desired reaction took place with monophosphines such as PCy_3 (entry 13). No catalytic activity was observed using $AlCl_3$ in place of $AlMe_3$, even when using the CoI_2/Zn combination to ensure the reduction of the Co precatalyst (entry 14). Meanwhile, $Zn(OTf)_2$ and $Ti(OiPr)_4$ promoted the hydrocarbamoylation albeit with much reduced efficiency (entries 15 and 16), suggesting Co/Zn and Co/Ti cooperations in the C–H activation. While all the experiments shown in Table 1 (and hereafter) were set up in a glove box, the present catalytic system did not actually need such a facility. Thus, the reaction in entry 8 could be performed outside the glove box using the standard Schlenk technique, without apparent decrease in the efficiency (93% yield).

Table 1. Addition of DMF to 5-Decyne under Co and Co/Al Catalysis[a]

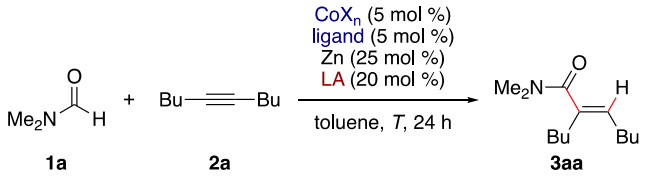

1a **2a** **3aa**

entry	CoX_n	ligand[b]	LA	*T* (°C)	yield (%)[c]
1[d]	CoI_2	dppp	none	100	71
2[d,e]	CoI_2	dppp	none	100	99
3	CoI_2	dppp	none	60	0
4	CoI_2	dppp	$AlMe_3$	60	99 (96)
5	$CoBr_2$	dppp	$AlMe_3$	60	83
6	$CoCl_2$	dppp	$AlMe_3$	60	99
7	$Co(acac)_3$	dppp	$AlMe_3$	60	91
8[f]	$Co(acac)_3$	dppp	$AlMe_3$	60	99 (96)
9[f]	$CoCl(PPh_3)_3$	dppp	$AlMe_3$	60	88
10[f,g]	$Co_2(CO)_8$	dppp	$AlMe_3$	60	0
11[f]	$Co(acac)_3$	dppb	$AlMe_3$	60	32
12[f]	$Co(acac)_3$	dppbz	$AlMe_3$	60	76
13[f,h]	$Co(acac)_3$	PCy_3	$AlMe_3$	60	0
14	CoI_2	dppp	$AlCl_3$	60	0
15	CoI_2	dppp	$Zn(OTf)_2$	60	25
16	CoI_2	dppp	$Ti(OiPr)_4$	60	27

[a]Unless otherwise noted, the reaction was performed using 0.4 mmol of **1a** and 0.2 mmol of **2a** in toluene (0.3 mL). [b]dppp = 1,3-bis(diphenylphosphino)propane; dppe = 1,2-bis(diphenylphosphino)ethane; dppbz = 1,2-bis(diphenylphosphino)benzene. [c]Determined by GC using *n*-tridecane as an internal standard. Isolated yield is shown in parentheses. [d]The reaction was performed in DMF (0.3 mL) instead of toluene, using 2.5 mol % each of CoI_2 and dppp. [e]DABCO (25 mol %) was added. [f]The reaction was performed in heptane instead of toluene, in the absence of Zn. [g]2.5 mol % of $Co_2(CO)_8$ was used. [h]10 mol % of PCy_3 was used.

With the effective Co/Al catalytic systems in hand, we explored the scope of formamides and alkynes (Table 2). A variety of acyclic and cyclic *N*,*N*-dialkylformamides participated in the addition to **2a** to afford the corresponding α,β-unsaturated amides **3aa**–**3ia** in good yields with exclusive *syn*-selectivity, except for bulky *N*,*N*-diisopropylformamide that reacted sluggishly (see **3fa**). On the other hand, formamides bearing *N*-aryl substituent failed to participate in the desired reaction. Besides **2a**, symmetrical and unsymmetrical dialkylacetylenes underwent addition of **1a** to afford the corresponding products **3ab**–**3ad** in good yields. The reaction of 2,2-dimethyloct-3-yne took place with exclusive regioselectivity, with the C–C bond formation at the less hindered acetylenic carbon (see **3ad**). Phenyl cyclohexyl acetylene and vinyl cyclohexyl acetylene were also amenable to the hydrocarbamoylation, again with C–C bond formation at the less hindered acetylenic carbons (see **3ae** and **3af**). The regioselectivity trend observed for such unsymmetrical alkynes may be rationalized by the preference of the cobalt center to avoid a steric repulsion with the bulkier alkyne substituent during the LLHT process. The addition of **1a** to diphenylacetylene was also feasible, albeit with moderate yield and opposite stereoselectivity (see **3ag**). The reaction between **1a** and **2a** could be scaled up to 6 mmol scale, affording the adduct **3aa** in a preparatively useful yield (1.06 g, 84%).

Table 2. Co/Al-Catalyzed Addition of Formamides to Alkynes[a]

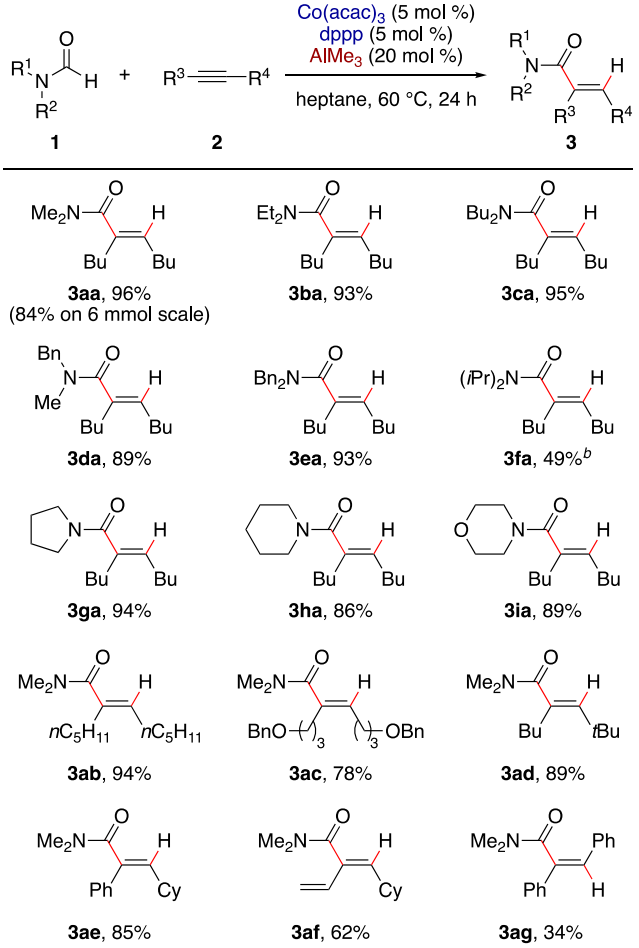

[a]Unless otherwise noted, the reaction was performed on a 0.2 mmol scale under the conditions in Table 1, entry 7. [b]Conditions: $Co(acac)_3$ (5 mol %), dppp (5 mol %), $AlMe_3$ (40 mol %), heptane, 100 °C, 72 h.

Scope of Co/LA Cooperative Catalysis for Hydrocarbofunctionalization of Alkynes. Having demonstrated the Co/Al-catalyzed hydrocarbamoylation of alkynes, we became interested in the generality of Co/LA systems for C–H activation as well as their potential uniqueness in comparison with the known Ni/LA catalytic systems. As such, we set out to explore the addition of a series of Lewis basic substrates to alkynes. First, we examined the reactivity of pyridone derivatives in light of their structural analogy to formamide. Coordination of the Lewis basic pyridone oxygen to a Lewis acid would give rise to a pyridinium-type species, which would possess intrinsically electron-deficient C4 and C6 positions (Scheme 2a). The Ni/Al catalytic system was reported to promote highly C6-selective alkenylation of *N*-methylpyridone (**4a**) with an alkyne, which was accompanied by a trace amount of C4, C6-dialkenylated product (Scheme 2b).[10a] By contrast, the Co/Al system was found to promote the activation of C4 and C6 positions of **4a** at comparable rates. Thus, using an excess amount (3 equiv) of **2a** with increased loadings of the cobalt catalyst (10 mol %) and $AlMe_3$ (40 mol %) at 100 °C, the dialkenylated product **5aa** was obtained in good yield. As expected from this observation, 6-substituted pyridone derivatives **4b** and **4c** underwent smooth C4-alkenylation with 5 mol % Co and 20 mol % Al at 100 °C to give **5ba** and **5ca** in good yields, while 4-substituted pyridone **4d** was also amenable to C6-alkenylation to afford **5da** in 68% yield. *N*-Methylpyrimidin-4-one (**4e**) and -quinolin-4-one (**4f**) also underwent site-selective C–H activation of the C2 position to afford the alkenylated products **5ea** and **5fa** in good yields. 1,3-Dimethyluracil (**4g**) proved particularly reactive, undergoing smooth C6-alkenylation at 80 °C in excellent yield (see **5ga**). 1,6-Dimethylpyridone (**4b**) reacted smoothly with *t*Bu-substituted unsymmetrical alkynes to afford the corresponding products **5bd** and **5bh** with exclusive regio- and stereoselectivity. Note that pyridone derivatives **4b**, **4c**, and **4f** have not been examined in the Ni/Al-catalyzed alkenylation reaction.[10a]

Scheme 2. Co/Al-Catalyzed Alkenylation of Pyridone Derivatives with Alkynes

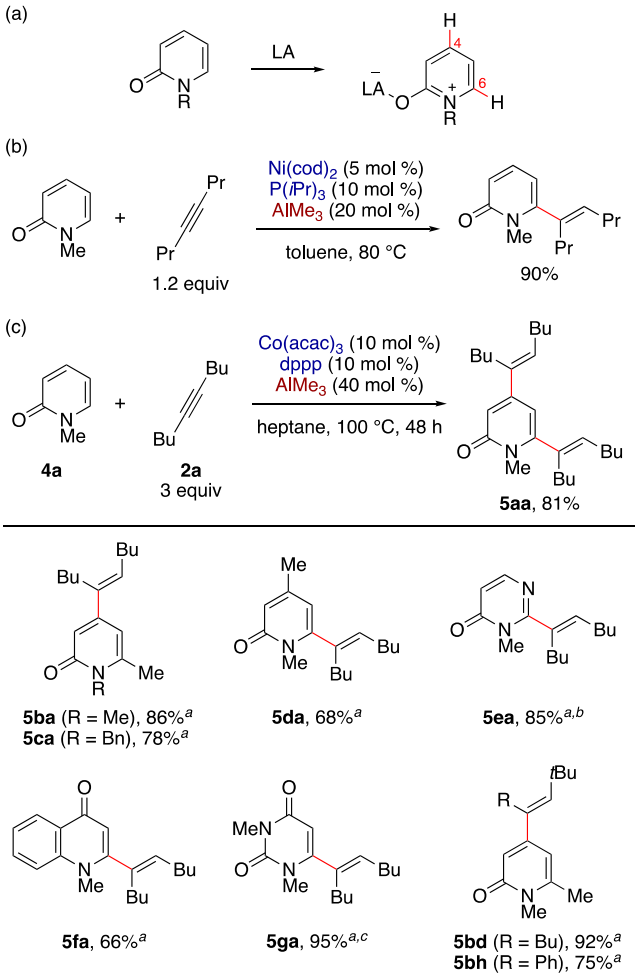

[a]The reaction was performed using 0.2 mmol pyridone derivative, 0.3 mmol alkyne, 5 mol % $Co(acac)_3$, 5 mol % dppp, and 20 mol % $AlMe_3$ in heptane at 100 °C for 24 h. [b]*E*/*Z* = 71:29. [c]The reaction was performed at 80 °C.

We next turned our attention to the activation of pyridine derivatives. Pyridine is an intrinsically electron-deficient aromatic system, and its complexation with a Lewis acid is expected to render it even more electron-deficient to enhance its reactivity toward electron-rich low-valent transition metal species, especially at the C2 and C4 positions (Scheme 3a). A few Ni/LA-based catalytic systems have been reported for the alkenylation of pyridine with alkynes (Scheme 3b). As mentioned in Introduction, Nakao and Hiyama demonstrated

exclusively C2-selective alkenylation of pyridine with alkynes using Ni(0)–trialkylphosphine catalyst and ZnR_2 (R = Me or Ph).[3] The use of $AlMe_3$ instead of ZnR_2 also resulted in site-selective C2 activation, while affording a dienylated product through incorporation of two alkyne molecules. Following this report, Ong and coworkers reported C4-selective alkenylation of pyridine using a Ni/Al catalytic system featuring a bifunctional NHC ligand.[6] Meanwhile, Nakao and Hiyama combined a Ni(0)–bulky NHC catalyst with a bulky aluminum Lewis acid, MAD ($(2,6\text{-}t\text{Bu-4-Me}C_6H_2O)_2AlMe$), to achieve C4-selective alkylation of pyridine with alkenes, while application of the Ni/MAD system to the alkenylation reaction was not described.[5] Instead, they briefly noted C4-selective alkenylation using a catalytic system comprised of $Ni(cod)_2$, 1,3-bis(2,4,6-trimethylphenyl)imidazol-2-ylidene (IMes), and $AlMe_3$. Nonetheless, these "C4-selective" alkenylation reactions were accompanied by substantial amount of the C3-alkenylation product.

With brief screening of reaction conditions for the cobalt-catalyzed reaction between pyridine (**6a**) and **2a** (see Table S7), we have found that a catalytic system comprised of $Co(acac)_3$ (5 mol %), dppp (5 mol %), and MAD (40 mol %) effects the C4-alkenylation reaction in heptane at 100 °C, affording the product **7aa** in 81% yield with exclusive site selectivity (Scheme 3c). The reaction could be performed on a 6 mmol scale in a comparable yield (78%). Using $AlMe_3$ (40 mol %) instead of MAD, the reaction still displayed selectivity toward the C4 position, affording the alkenylation products in an overall yield of 48% with the ratio of C2:C3:C4 = 5:13:82. By contrast, the use of $ZnMe_2$ (40 mol %) as the Lewis acid under otherwise identical conditions resulted in preferential C2-alkenylation, yet producing sizable amounts of C3- and C4-alkenylation products (overall yield 47%, C2:C3:C4 = 60:12:28). Thus, compared with Ni catalysts, the Co–dppp catalyst appeared to have intrinsic preference toward C4-activation, which would be reinforced by the bulky MAD that blocks the C2 and C3 positions. For 2-substituted pyridine derivatives, the reaction became sluggish with the Co/MAD system, but instead the use of $AlMe_3$ proved to efficiently promote C4-selective alkenylation to afford the alkenylated products **7ba**–**7ea** in good yields. Furthermore, 3-substituted pyridines also underwent C4-alkenylation with **2a** under Co/MAD or Co/$AlMe_3$ system (see **7fa** and **7ga**). The pyridine C4-alkenylation could also be performed using unsymmetrical dialkylalkynes or aryl alkyl alkynes, affording the products **7ad** and **7ah** in excellent yields.

Azine heterocycles other than pyridine, such as pyrimidine and pyrazine derivatives, also underwent the addition to 5-decyne under the Co/MAD system to afford the alkenylation products **7ha**–**7ja** in moderate to good yields, while pyridazine failed to participate in the reaction. Particularly noteworthy is the exclusive C4 selectivity observed for parent pyrimidine (see **7ha**). Meanwhile, given the C4 selectivity for pyridines, it was curious that the reaction of quinoline with **2a** took place exclusively at the C2 position even by using MAD as the Lewis acid, affording **7ka** in 66% yield.[3,6]

Scheme 3. Co/Al-Catalyzed Alkenylation of Pyridine Derivatives with Alkynes

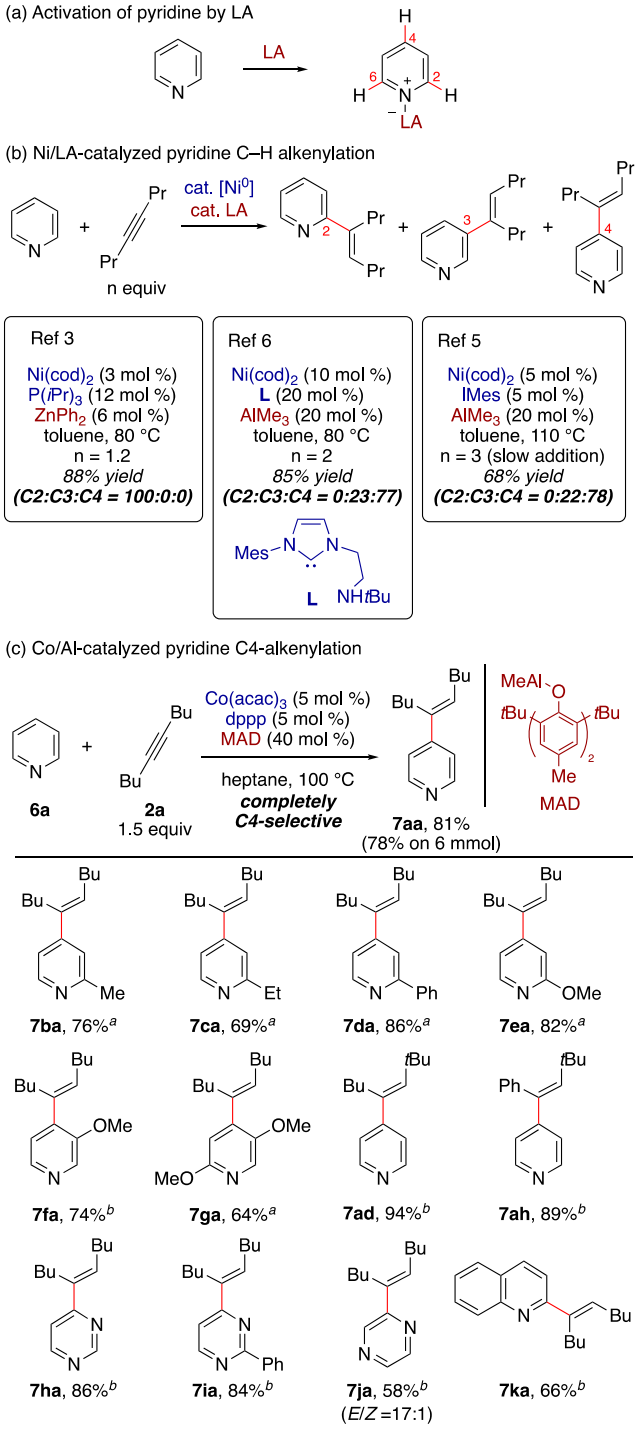

[a]The reaction was performed using 0.2 mmol pyridine derivative, 0.3 mmol alkyne, 5 mol % $Co(acac)_3$, 5 mol % dppp, and 40 mol % $AlMe_3$ in heptane at 100 °C for 24 h. [b]MAD (40 mol %) was used instead of $AlMe_3$.

With successful engagement of pyridine derivatives as substrates, we became interested in the reactivity of imidazo[1,2-*a*]pyridine, which is among important heterocyclic motifs in pharmaceuitcals,[31] under the Co/Al catalysis. We hypothesized that coordination of the nitrogen (position 1) to $AlMe_3$ would particularly reduce the electron density at the C3, C5, and C7 positions and thus enhance their reactivity toward C–H activation (Scheme 4 box). While the reaction of parent imidazo[1,2-*a*]pyridine with 5-decyne afforded an intractable

mixture of alkenylation products, 2-aryl- and alkyl-substituted imidazo[1,2-*a*]pyridines underwent exclusive C–H activation at the C5 position to afford the desired products **9aa**–**9ca** in good yields (Scheme 4). Unsymmetrical alkynes also participated in the reaction with 2-phenylimidazo[1,2-*a*]pyridine to afford the C5-alkenylation products **9ad**, **9af**, and **9ah** in moderate to good yields. While the preference for the C5 position to the C3 and C7 positions remains unclear, the present alkenylation represents a rare example of C5-selective functionalization of imidazo[1,2-*a*]pyridines.[31,32]

Scheme 4. Co/Al-Catalyzed Alkenylation of Imidazo[1,2-*a*]pyridine Derivatives

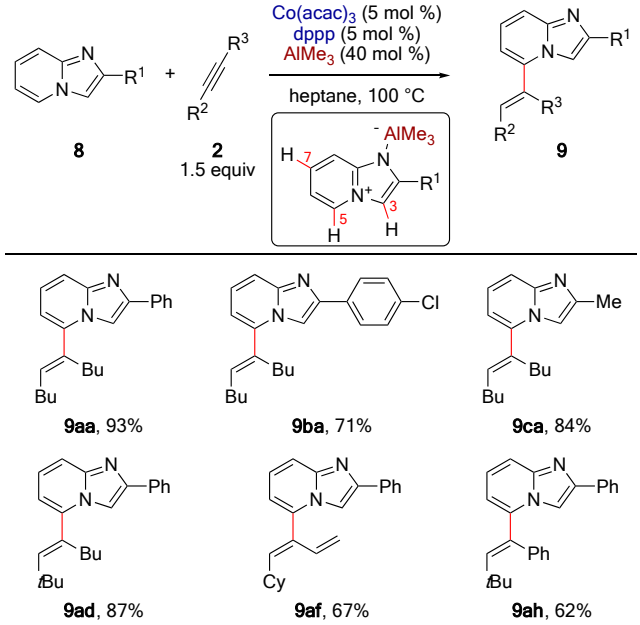

[a]The reaction was performed using 0.2 mmol imidazo[1,2-*a*]pyridine derivative, 0.3 mmol alkyne, 5 mol % $Co(acac)_3$, 5 mol % dppp, and 40 mol % $AlMe_3$ in heptane at 100 °C for 24 h.

On extending the substrate scope of the Co/Al catalytic systems, our attention came back to the C2-alkenylation of oxazole and thiazole derivatives. While such transformation was achieved using Ni(0)–trialkylphosphine catalysts[18] as well as Co–diphosphine catalysts combined with Grignard reductant (Scheme 2a),[20] we were interested in the feasibility of the Co/LA cooperative C–H activation of this class of substrates. The present standard catalytic system ($Co(acac)_3$/dppp/$AlMe_3$) proved effective for the C2-alkenylation of (benzo)thiazole derivatives (Scheme 5). Thus, benzothiazole (**10a**) underwent *syn*-selective addition to a series of internal alkynes to afford the corresponding adducts **11af**, **11ag**, **11ai**, and **11aj** in high yields. The reaction of **10a** with an unsymmetrical diaryl alkyne bearing methoxy and ethoxycarbonyl groups at the *para*-positions gave a mixture of regioisomers **11ak** and **11ak'** in 82% overall yield with a ratio of ca. 3:1, with preferential C–C bond formation at the acetylenic carbon proximal to the electron-deficient aryl group. Parent and methyl-substituted thiazoles were also amenable to C2-alkenylation with diphenylacetylene, affording the products **11bg**–**11dg** in good yields with high *E*/*Z* ratios. The role of $AlMe_3$ as Lewis acid to activate the thiazole nitrogen (as well as reductant) was supported by a control experiment using Zn instead of $AlMe_3$, which did not produce the desired alkenylation product.

Scheme 5. Co/Al-Catalyzed Alkenylation of (Benzo)thiazoles

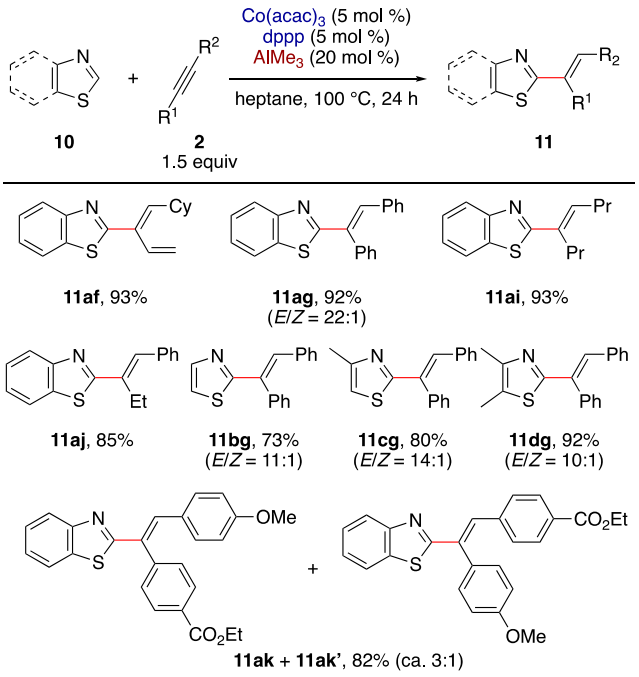

[a]The reaction was performed using 0.2 mmol (benzo)thiazole derivative, 0.3 mmol alkyne, 5 mol % $Co(acac)_3$, 5 mol % dppp, and 20 mol % $AlMe_3$ in heptane at 100 °C for 24 h. The *E*/*Z* ratio was determined by GC analysis.

Unexpectedly, analogous C2-alkenylation of 5-methylbenzoxazole (**12a**) with 4-octyne (**2i**) proceeded rather sluggishly using the above standard catalytic system. Upon re-optimization of reaction conditions (Table S8), a Co/Ti combination proved effective (Scheme 6). Thus, a catalytic system comprised of CoI_2 (5 mol %), dppp (5 mol %), Zn (25 mol %), and $Ti(OiPr)_4$ (20 mol %) promoted the desired C2-alkenylation between **12a** and **2i** in DME at 100 °C, affording the product **13ai** in good yield. Zn and $Ti(OiPr)_4$ would serve as reductant and Lewis acid, respectively, as no reaction was observed in the absence of either. The generality of the Co/Ti system was briefly demonstrated using a few different benzoxazole derivatives and alkynes, affording the desired products in moderate to high yields with *syn*-selectivity (Scheme 6).[33]

Scheme 6. Co/Ti-Catalyzed Alkenylation of Benzoxazoles

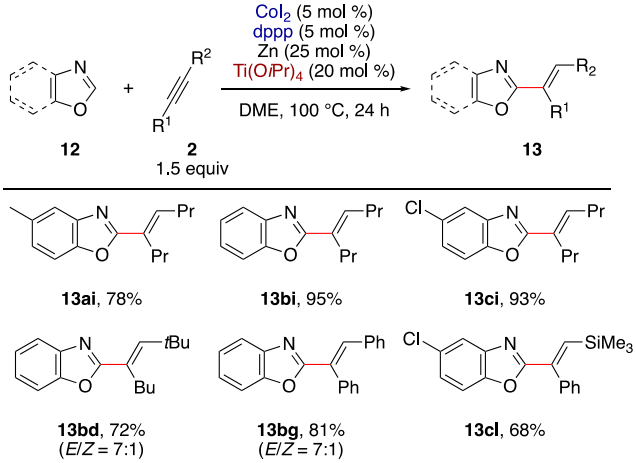

[a]The reaction was performed using 0.2 mmol benzoxazole derivative, 0.3 mmol alkyne, 5 mol % CoI_2, 5 mol % dppp, 25 mol % Zn, and 20 mol % $Ti(OiPr)_4$ in DME at 100 °C for 24 h. The *E*/*Z* ratio was determined by GC analysis.

Mechanistic Studies. To gain insight into the working mode of the Co/LA catalytic systems, we performed mechanistic experiments and DFT calculations on the hydrocarbamoylation of alkyne. The reaction of deuterated DMF (**1a**-d_7) with **2a** under the standard conditions afforded the product **3aa**-d_7 in 79% yield, with clean transfer of the carbamoyl deuterium of **1a**-d_7 to the vinylic position (Scheme 7a). A crossover experiment using a mixture of **1a**-d_7 and nondeuterated formamide **1d** afforded **3aa**-d_7 and **3da** without any H/D crossover, demonstrating that the carbamoyl group and the hydrogen (or deuterium) atom of the product originate from the same formamide molecule (Scheme 7b). The comparison of initial rates of individual reactions of **1a** and **1a**-d_7 gave H/D kinetic isotope effect (KIE) of 2.5 (average of two sets of experiments), indicating that C–H bond cleavage would be involved in the rate-limiting step of the reaction (Scheme 7c). Furthermore, an intermolecular competition reaction using a mixture of **1a** and **1a**-d_7 gave KIE of similar magnitude (3.0; average of two runs), which would have also reflected the C–H cleavage as the step of first irreversible conversion of formamide (Scheme 7d).

Scheme 7. Deuterium-Labeling and KIE Experiments

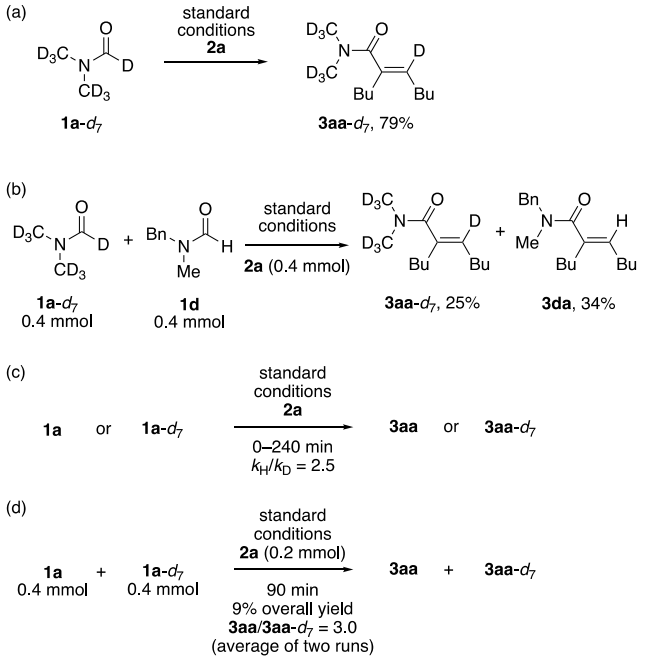

We next explored possible reaction pathways of the Co/Al-catalyzed hydrocarbamoylation by DFT calculations using simple model systems, assuming that Co(II) or Co(III) precatalyst, in the presence of diphosphine ligand, is reduced by $AlMe_3$ to generate a cationic (diphosphine)Co(I) species. Note that such species have been often proposed to be generated in catalytic systems comprised of Co(II)–diphosphine complexes and alkylaluminum reagents (e.g., $AlMe_3$, Et_2AlCl, MAO) for C–C bond forming reactions such as cycloaddition and hydrovinylation, where the alkylaluminum would act as a reductant as well as an anion abstractor,[34] while species of different oxidation state, such as (diphosphine)Co(0), may not be excluded depending on the reducing agent and the reaction conditions.[35] Thus, the reaction of DMF and 2-butyne with $[(dppp)Co]^+$ was probed in the absence or presence of $AlMe_3$.[36]

Reaction pathways and energy diagrams for the model Co- and Co/Al-catalyzed hydrocarbamoylation are summarized in Figure 1a and 1b, respectively. Note that the suffixes **s** and **t** on the structure numberings refer to the singlet and triplet states, respectively. First, reaction pathways in the absence of $AlMe_3$ were probed (Figure 1a). The cationic $[(dppp)Co]^+$ prefers to bind one molecule of DMF and one molecule of alkyne to form the complex **CP1_t**. A bis-alkyne complex **CP2_t** and a bis-DMF complex **CP3_t** were calculated to be less stable by 6.6 and 0.9 kcal mol^{-1}, respectively (Figure S6). Furthermore, their singlet counterparts **CP1_s**, **CP2_s**, and **CP3_s** were calculated to be even less stable (ΔG = 12.1, 16.4, and 23.9 kcal mol^{-1}, respectively). **CP1_t** may be connected to **CP1_s** by minimum energy crossing point (MECP) with ΔG of 12.0 kcal/mol (**MECP1**). The following C–H bond cleavage was found to take place through a ligand-to-ligand hydrogen transfer (LLHT) transition state,[11,25,37] where the Co–carbamoyl bond, the Co–alkenyl bond, and the vinylic C–H bond form in a concerted fashion. Here, the singlet TS (**TS1_s**, ΔG = 36.0 kcal/mol) was found to be lower in energy than the triplet TS (**TS1_t**, ΔG = 38.1 kcal/mol). The resulting diorganocobalt intermediates **INT1_s** and **INT1_t** are less stable (ΔG = 16.8 and 16.6 kcal mol^{-1}, respectively) than the starting complexes, and are connected by **MECP2** with ΔG of 26.0 kcal mol^{-1}. The

following reductive elimination preferentially occurs in the triplet state (**TS2_t**, ΔG = 20.3 kcal mol^{-1}) than in the singlet state (**TS2_s**, ΔG = 31.7 kcal mol^{-1}), forming the product complex **INT2_t** (ΔG = –13.7 kcal mol^{-1}). **INT2_t** may undergo ligand exchange with DMF and 2-butyne to liberate the α,β-unsaturated amide product and regenerate the starting complex **CP1_t**. Overall, LLHT (**TS1_t**) was found to be the step of the highest activation barrier ($\Delta G^{\ddagger}$ = 36.0 kcal mol^{-1}). Although energetically uphill, LLHT might be practically irreversible as the following process (from **INT1_s** to **TS2_t**) might be faster than reverse-LLHT.

Besides the LLHT pathway, we have also found a stepwise reaction pathway involving carbamoyl C–H oxidative addition and subsequent migratory insertion of the alkyne into the Co–H bond on the singlet surface, which converges to **INT1_s** (Figure S7a). However, C–H oxidative addition, the highest-energy step in this stepwise pathway, was found to require a higher activation energy than LLHT by 3.3 kcal mol^{-1}. Note that our attempts to locate a C–H oxidative addition TS on the triplet surface failed and converged to the triplet LLHT TS. Meanwhile, we could locate the oxidative addition product, the migratory insertion TS, and the migratory insertion product on the quintet surface, but they were significantly higher in energy than their singlet counterparts.

Next, we introduced $AlMe_3$ to the system to probe its influence on the energy landscape. $AlMe_3$ coordinates to the oxygen atom of **CP1_t** to form the bimetallic complex **CP1a_t**, with stabilization by 0.8 kcal mol^{-1}. While the corresponding singlet complex **CP1a_s** is not particularly stabilized, the LLHT TS, **TS1a_s**, is highly stabilized by $AlMe_3$ coordination (ΔG = 28.7 kcal mol^{-1}). The following diorganocobalt species **INT1a_s** and **INT1a_t** are also much stabilized by $AlMe_3$ coordination, compared with their Al-free counterparts (**INT1_s** and **INT1_t**). The triplet reductive elimination TS (**TS2a_t**) is also greatly stabilized (ΔG = 12.8 kcal mol^{-1}), leading to the Co/Al-bound product **INT2a_t**. Again, the LLHT step was found to require the highest activation energy ($\Delta G^{\ddagger}$ = 29.5 kcal mol^{-1}), which was much lower (by 6.5 kcal mol^{-1}) than the barrier for the Al-free pathway. We also located C–H oxidative addition TS involving $AlMe_3$, which was less stable than **TS1a_s** by 7.3 kcal mol^{-1} (Figure S7b). This significant energy gap suggests that the present Co/Al catalysis is likely to operate by LLHT mechanism rather than the stepwise oxidative addition–migratory insertion mechanism.

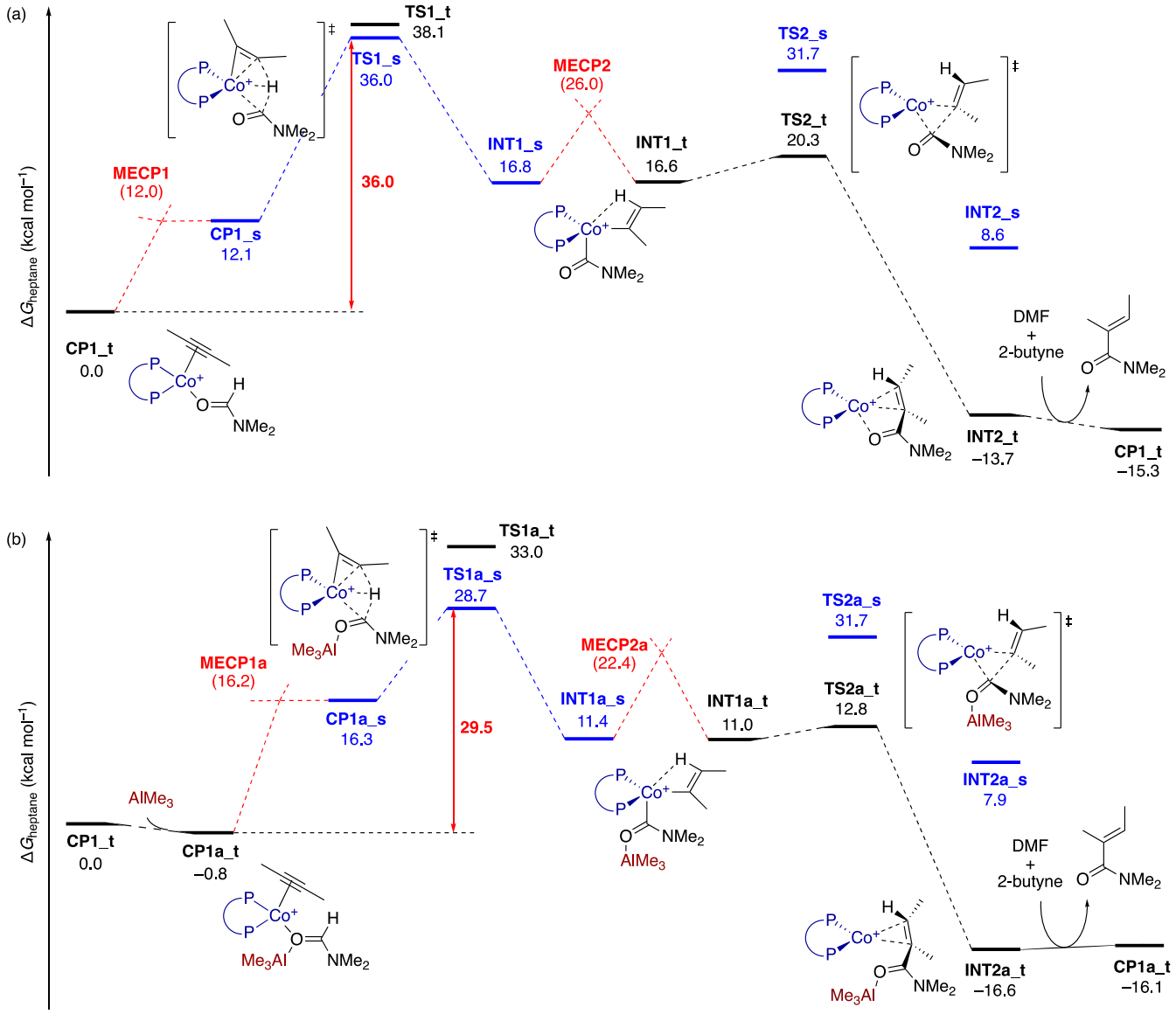

Figure 1. Gibbs free energy diagram of the addition of DMF to 2-butyne promoted by $[Co(dppp)]^+$ in the (a) absence and (b) presence of $AlMe_3$ calculated at SMD(heptane)-M06L/6-311++G(2df,2p)-SDD(Co)//M06L/6-31G(d)-SDD(Co) level.

Figure 2 shows the 3-D structures of the precursor complexes and LLHT TSs in the absence (**CP1_s** and **TS1_s**) and presence (**CP1a_s** and **TS1a_s**) of $AlMe_3$. An obvious difference between **CP1_s** and **CP1a_s** can be found in the Co–O distance (2.13 Å in **CP1_s** and 2.48 Å in **CP1a_s**). The longer Co–O distance in the latter can be attributed to the competition between Co and Al in the coordination to the amide oxygen, where Al apparently serves as a stronger Lewis acid with the Al–O distance of 2.04 Å. While directly leading to the alkenyl(carbamoyl)cobalt intermediates (**INT1_s** and **INT1a_s**), both the TS structures at a glance appear like C–H oxidative addition TSs. Thus, they both feature short Co–C^1 (carbonyl carbon; ca. 2.0 Å) and Co–H (ca. 1.5 Å) distances and substantially elongated C^1–H bond (1.60–1.72 Å). The significant development of the Co–C^1 bond in these TSs is also seen from wide Co–C^1–O–N dihedral angles (>170°; ca. 179° in **INT1_s** and **INT1a_s**). The acetylenic carbons C^2 and C^3 have similar distances from the Co center (ca. 1.9 Å), and the formation of the C^2–H bond is rather premature (ca. 2.2 Å).

Between the Al-free and the Al-containing LLHT TSs, **TS1a_s** apparently features more advanced Co–C^1 bond formation and C^1–H^1 bond cleavage than **TS1_s**, as judged from the distinctly shorter Co–C^1 distance (by 0.04 Å) and longer C^1–H^1 distance (by 0.12 Å). These structural features agree with the Mayer bond orders[38,39] of the Co–C^1 (0.835 in **TS1a_s** vs 0.764 in **TS1_s**) and the C^1–H^1 (0.133 in **TS1a_s** vs 0.178 in **TS1_s**) bondings. The Mayer bond orders also demonstrate that the temporary Co–H^1 bonding is stronger in **TS1a_s** (0.696) than in **TS1_s** (0.651) and that the bonding between C^2 and H^1 is barely developed (ca. 0.035 for both TSs). These differences may be qualitatively attributed to the role of $AlMe_3$ to reduce the electron density of DMF and thereby to facilitate greater charge transfer from the cobalt catalyst. This notion is in line with atomic-dipole-moment-corrected Hirshfeld (ADCH) atomic charges,[39,40] which show that 1) $AlMe_3$ coordination makes the DMF segment more positively charged, 2) the positive charge of the DMF segment decreases toward the LLHT TS, and 3) the dppp–Co segment has greater positive charge in **TS1a_s** than in **TS1_s**.

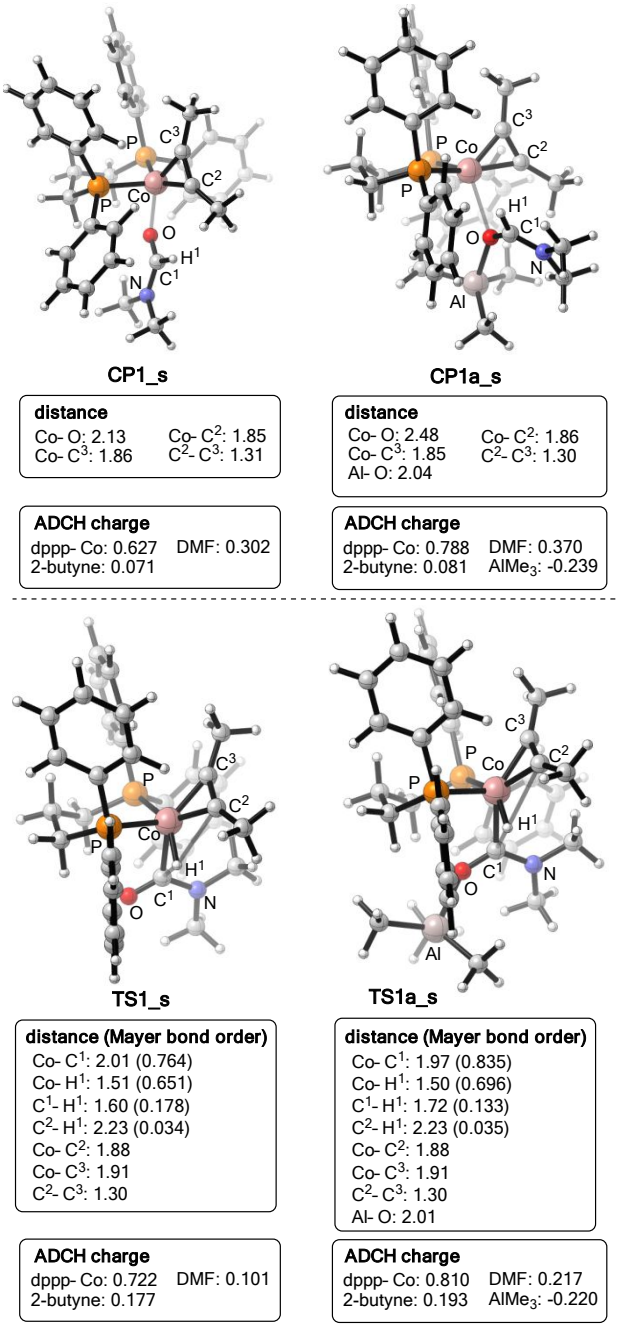

Figure 2. Precursor complexes and transition states of the LLHT step. The distances are in Å.

To probe the origin of $AlMe_3$ effect on the activation barriers of the LLHT process, distortion/interaction analysis[41] on the precursor complexes (**CP1_s** and **CP1a_s**) and the LLHT TSs (**TS1_s** and **TS1a_s**) was performed by separating these structures into Co–alkyne and DMF(–$AlMe_3$) segments (Scheme 8). The activation energy of 24.4 kcal mol^{-1} from **CP1_s** to **TS1_s** was decomposed into interaction energy in **CP1_s** (–28.6 kcal mol^{-1}), distortion energies of the Co–alkyne segment (9.7 kcal mol^{-1}) and the DMF segment (54.0 kcal mol^{-1}), and interaction energy in **TS1_s** (–67.9 kcal mol^{-1}) (Scheme 8a). The same analysis on **CP1a_s** and **TS1a_s** revealed that the distortion energy of the Co–alkyne fragment

is comparable, while the other three components are substantially different (Scheme 8b). Thus, the larger distortion energy of the DMF–$AlMe_3$ segment (66.3 kcal mol^{-1}) is overwhelmed by the combination of the larger interaction energy in **TS1a_s** (–81.3 kcal mol^{-1}) and the smaller interaction energy in **CP1a_s** (–20.9 kcal mol^{-1}), resulting in the lower overall activation energy (16.6 kcal mol^{-1}). The larger interaction energy in **TS1a_s** appears to be the consequence of the DMF activation by $AlMe_3$, while the smaller interaction energy in **CP1a_s** can be ascribed to the weakening of the Co–O interaction (compared to that in **CP1_s**) caused by the strong Al–O coordination.

Scheme 8. Distortion/Interaction Analysis[a]

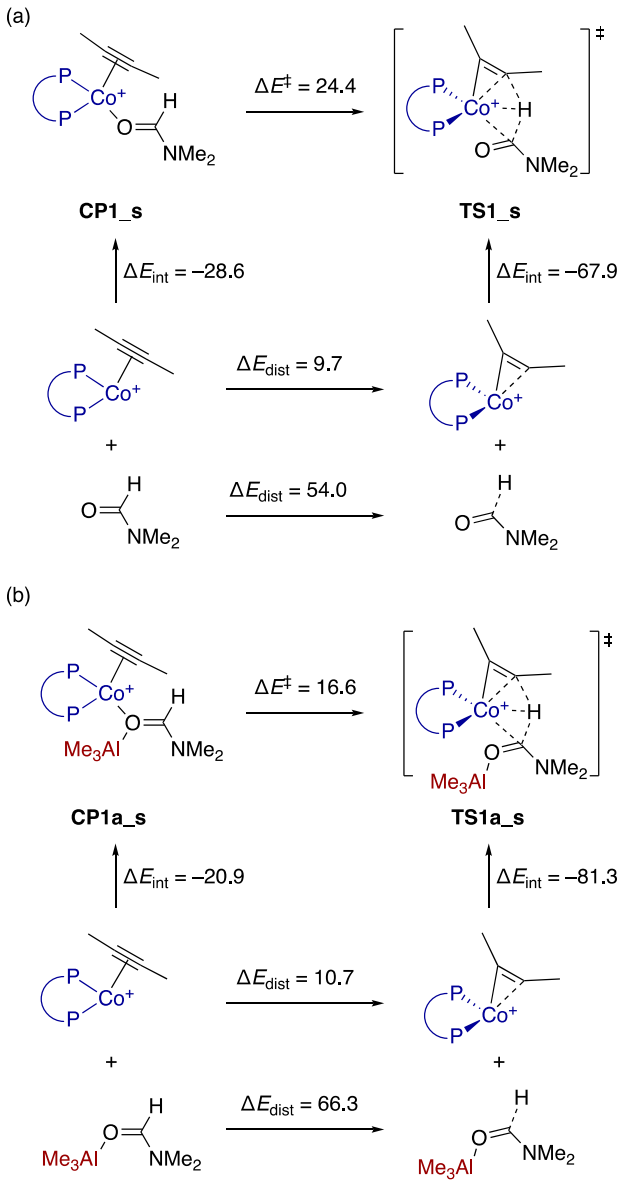

[a]Energies refer to the electronic energies (kcal mol^{-1}) calculated at SMD(heptane)-M06L/6-311++G(2df,2p)-SDD(Co)//M06L/6-31G(d)-SDD(Co) level. ΔE_{dist} and ΔE_{int} refer to distortion and interaction energies, respectively.

We also performed distortion/interaction analysis by different fragmentation scheme (i.e., fragmentation into Co–alkyne–DMF segment and $AlMe_3$ segment) to probe how **CP1_s** and **TS1_s** are stabilized by coordination of $AlMe_3$ to yield **CP1a_s** and **TS1a_s**, respectively (see Scheme S1). This analysis revealed that the Co–alkyne–DMF segment in **TS1a_s** is distorted from that in **TS1_s** by only 2.7 kcal mol^{-1}, which is consistent with the roughly similar core structures of **TS1_s** and **TS1a_s** (Figure 2). By contrast, the same segment in **CP1a_s** is more distorted from that in **CP1_s** (by 13.5 kcal mol^{-1}), reflecting the significant elongation of the Co–O distance. As the interaction energy between the Co–alkyne–DMF segment and the $AlMe_3$ segment is calculated to be larger for **CP1a_s** (–32.5 kcal mol^{-1}) than for **TS1a_s** (–30.3 kcal mol^{-1}), the difference in the distortion energies appears to contribute significantly to the overall greater stabilization of **TS1_s** toward **TS1a_s** (–21.6 kcal mol^{-1}) than that of **CP1_s** toward **CP1a_s** (–13.8 kcal mol^{-1}).

CONCLUSION

In summary, we have demonstrated that Co/LA catalytic systems promote hydrocarbofunctionalization of alkynes with Lewis basic and electron-deficient substrates via cooperative C(sp^2)–H activation. The combination of a cobalt–dppp complex and an aluminum Lewis acid such as $AlMe_3$ or MAD proved particularly effective, promoting the reaction of formamides, pyridones, pyridines and related azines, imidazo[1,2-*a*]pyridines, and thiazole derivatives, while a titanium Lewis acid ($Ti(OiPr)_4$) was found to be uniquely effective for oxazole derivatives. The Co/LA systems would serve as alternative or complementary systems to the known Ni/LA systems, and the present study has thus far revealed some practically or mechanistically notable features. First, the present systems are easy to set up using readily available, bench-stable and inexpensive cobalt precatalysts ($Co(acac)_3$ or CoI_2) as well as common diphosphine ligand (dppp). Given that most of the Ni/LA systems employ electron-rich, air-sensitive, and sometimes pyrophoric monodentate ligands such as trialkylphosphines or NHCs, the effectiveness of dppp in the Co/LA systems not only represents a practical merit but also provides a valuable opportunity for further improvement and design of catalysts through exploration of the vast chemical space of bidentate ligands. Second, the Co/Al catalytic systems display unique site selectivity toward substrates such as pyridone and pyridine derivatives. While the C4 and C6 positions of pyridone have proven to be equally reactive toward the Co/Al catalyst, completely C4-selective alkenylation of pyridine has been achieved for the first time. The origin of such distinct site selectivity remains to be seen. In this context, the exclusive selectivity toward the C5 position of imidazo[1,2-*a*]pyridines is also intriguing. Lastly, the mechanistic study suggested that the present C–H activation reaction proceeds via LLHT, which represents a commonly proposed mechanism for Ni- and Ni/LA-catalyzed hydrocarbofunctionalization of alkenes and alkynes. This mechanistic insight may imply that the parallelism between low-valent Ni and Co is not superficial but is based on fundamental common reactivity shared by these 3d transition metals,[42] which would warrant further synthetic and mechanistic explorations.

ASSOCIATED CONTENT

Supporting Information

The Supporting Information is available free of charge on the ACS Publications website.

Experimental procedures, spectral data for all new compounds and computational details (PDF)

Crystallographic data for **11ck** (CIF)

AUTHOR INFORMATION

Corresponding Author

*E-mail: wangchen@usx.edu.cn
*E-mail: nyoshikai@ntu.edu.sg

Present Addresses

[§]Department of Chemistry, University of Warwick, CV4 7AL Coventry, United Kingdom.
[‖]Faculty of Chemistry, VNU University of Science, Vietnam National University, Hanoi, Vietnam.

ACKNOWLEDGMENT

This work was supported by the Singapore Ministry of Education Academic Research Fund Tier 2 (MOE2016-T2-2-043 to N.Y.) and Tier 1 (RG114/18 to N.Y.), Zhejiang Provincial Natural Science Foundation of China (Grant No. LY18B020007 to C.W.), and Nanyang Technological University. We thank Dr. Yongxin Li (Nanyang Technological University) for his assistance with the X-ray crystallographic analysis.

REFERENCES

(1) (a) Kakiuchi, F.; Murai, S. Catalytic C-H/Olefin Coupling. *Acc. Chem. Res.* **2002**, *35*, 826-834. (b) Ritleng, V.; Sirlin, C.; Pfeffer, M. Ru-, Rh-, and Pd-Catalyzed C-C Bond Formation Involving C-H Activation and Addition on Unsaturated Substrates: Reactions and Mechanistic Aspects. *Chem. Rev.* **2002**, *102*, 1731-1770. (c) Foley, N. A.; Lee, J. P.; Ke, Z.; Gunnoe, T. B.; Cundari, T. R. Ru(II) Catalysts Supported by Hydridotris(Pyrazolyl)Borate for the Hydroarylation of Olefins: Reaction Scope, Mechanistic Studies, and Guides for the Development of Improved Catalysts. *Acc. Chem. Res.* **2009**, *42*, 585-597. (d) Colby, D. A.; Bergman, R. G.; Ellman, J. A. Rhodium-Catalyzed C-C Bond Formation Via Heteroatom-Directed C-H Bond Activation. *Chem. Rev.* **2010**, *110*, 624-655. (e) Arockiam, P. B.; Bruneau, C.; Dixneuf, P. H. Ruthenium(II)-Catalyzed C-H Bond Activation and Functionalization. *Chem. Rev.* **2012**, *112*, 5879-5918. (f) Dong, Z.; Ren, Z.; Thompson, S. J.; Xu, Y.; Dong, G. Transition-Metal-Catalyzed C-H Alkylation Using Alkenes. *Chem. Rev.* **2017**, *117*, 9333-9403.

(2) Nakao, Y. Hydroarylation of Alkynes Catalyzed by Nickel. *Chem. Rec.* **2011**, *11*, 242-251.

(3) Nakao, Y.; Kanyiva, K. S.; Hiyama, T. A Strategy for C-H Activation of Pyridines: Direct C-2 Selective Alkenylation of Pyridines by Nickel/Lewis Acid Catalysis. *J. Am. Chem. Soc.* **2008**, *130*, 2448-2449.

(4) Nakao, Y. Transition-Metal-Catalyzed C–H Functionalization for the Synthesis of Substituted Pyridines. *Synthesis* **2011**, 3209-3219.

(5) Nakao, Y.; Yamada, Y.; Kashihara, N.; Hiyama, T. Selective C-4 Alkylation of Pyridine by Nickel/Lewis Acid Catalysis. *J. Am. Chem. Soc.* **2010**, *132*, 13666-13668.

(6) Tsai, C.-C.; Shih, W.-C.; Fang, C.-H.; Li, C.-Y.; Ong, T.-G.; Yap, G. P. Bimetallic Nickel Aluminum Mediated Para-Selective Alkenylation of Pyridine: Direct Observation of η^2,η^1-Pyridine Ni(0)-Al(III) Intermediates Prior to C-H Bond Activation. *J. Am. Chem. Soc.* **2010**, *132*, 11887-11889.

(7) Kanyiva, K. S.; Löbermann, F.; Nakao, Y.; Hiyama, T. Regioselective Alkenylation of Imidazoles by Nickel/Lewis Acid Catalysis. *Tetrahedron Lett.* **2009**, *50*, 3463-3466.

(8) (a) Shih, W.-C.; Chen, W.-C.; Lai, Y.-C.; Yu, M.-S.; Ho, J.-J.; Yap, G. P. A.; Ong, T.-G. The Regioselective Switch for Amino-Nhc Mediated C-H Activation of Benzimidazole Via Ni-Al Synergistic Catalysis. *Org. Lett.* **2012**, *14*, 2046-2049. (b) Lee, W.-C.; Wang, C.-H.; Lin, Y.-H.; Shih, W.-C.; Ong, T.-G. Tandem Isomerization and C-H Activation: Regioselective Hydroheteroarylation of Allylarenes. *Org. Lett.* **2013**, *15*, 5358-5361.

(9) (a) Nakao, Y.; Idei, H.; Kanyiva, K. S.; Hiyama, T. Hydrocarbamoylation of Unsaturated Bonds by Nickel/Lewis-Acid Catalysis. *J. Am. Chem. Soc.* **2009**, *131*, 5070-5071. (b) Miyazaki, Y.; Yamada, Y.; Nakao, Y.; Hiyama, T. Regioselective Hydrocarbamoylation of 1-Alkenes. *Chem. Lett.* **2012**, *41*, 298-300. (c) Nakao, Y.; Morita, E.; Idei, H.; Hiyama, T. Dehydrogenative [4 + 2] Cycloaddition of Formamides with Alkynes through Double C-H Activation. *J. Am. Chem. Soc.* **2011**, *133*, 3264-3267.

(10) (a) Nakao, Y.; Idei, H.; Kanyiva, K. S.; Hiyama, T. Direct Alkenylation and Alkylation of Pyridone Derivatives by Ni/$AlMe_3$ Catalysis. *J. Am. Chem. Soc.* **2009**, *131*, 15996-15997. (b) Tamura, R.; Yamada, Y.; Nakao, Y.; Hiyama, T. Alkylation of Pyridone Derivatives by Nickel/Lewis Acid Catalysis. *Angew. Chem. Int. Ed.* **2012**, *51*, 5679-5682.

(11) Okumura, S.; Tang, S.; Saito, T.; Semba, K.; Sakaki, S.; Nakao, Y. Para-Selective Alkylation of Benzamides and Aromatic Ketones by Cooperative Nickel/Aluminum Catalysis. *J. Am. Chem. Soc.* **2016**, *138*, 14699-14704.

(12) Okumura, S.; Nakao, Y. Para-Selective Alkylation of Sulfonylarenes by Cooperative Nickel/Aluminum Catalysis. *Org. Lett.* **2017**, *19*, 584-587.

(13) (a) Donets, P. A.; Cramer, N. Ligand-Controlled Regiodivergent Nickel-Catalyzed Annulation of Pyridones. *Angew. Chem. Int. Ed.* **2015**, *54*, 633-637. (b) Diesel, J.; Finogenova, A. M.; Cramer, N. Nickel-Catalyzed Enantioselective Pyridone C-H Functionalizations Enabled by a Bulky N-Heterocyclic Carbene Ligand. *J. Am. Chem. Soc.* **2018**, *140*, 4489-4493.

(14) Wang, Y.-X.; Qi, S.-L.; Luan, Y.-X.; Han, X.-W.; Wang, S.; Chen, H.; Ye, M. Enantioselective Ni-Al Bimetallic Catalyzed Exo-Selective C-H Cyclization of Imidazoles with Alkenes. *J. Am. Chem. Soc.* **2018**, *140*, 5360-5364.

(15) Loup, J.; Muller, V.; Ghorai, D.; Ackermann, L. Enantioselective Aluminum-Free Alkene Hydroarylations through C-H Activation by a Chiral Nickel/JoSPOphos Manifold. *Angew. Chem. Int. Ed.* **2019**, *58*, 1749-1753.

(16) Zhang, W.-B.; Yang, X.-T.; Ma, J.-B.; Su, Z.-M.; Shi, S.-L. Regio- and Enantioselective C-H Cyclization of Pyridines with Alkenes Enabled by a Nickel/N-Heterocyclic Carbene Catalysis. *J. Am. Chem. Soc.* **2019**, *141*, 5628-5634.

(17) (a) Wozniak, L.; Cramer, N. Enantioselective C–H Bond Functionalizations by 3d Transition-Metal Catalysts. *Trends Chem.* **2019**, *1*, 471-484. (b) Loup, J.; Dhawa, U.; Pesciaioli, F.; Wencel-Delord, J.; Ackermann, L. Enantioselective C-H Activation with Earth-Abundant 3d Transition Metals. *Angew. Chem. Int. Ed.* **2019**, *58*, 12803-12818.

(18) (a) Nakao, Y.; Kanyiva, K. S.; Oda, S.; Hiyama, T. Hydroheteroarylation of Alkynes under Mild Nickel Catalysis. *J. Am. Chem. Soc.* **2006**, *128*, 8146-8147. (b) Kanyiva, K. S.; Nakao, Y.; Hiyama, T. Practical Approach for Hydroheteroarylation of Alkynes Using Bench-Stable Catalyst. *Heterocycles* **2007**, *72*, 677-680.

(19) Mukai, T.; Hirano, K.; Satoh, T.; Miura, M. Nickel-Catalyzed C-H Alkenylation and Alkylation of 1,3,4-Oxadiazoles with Alkynes and Styrenes. *J. Org. Chem.* **2009**, *74*, 6410-6413.

(20) (a) Ding, Z.; Yoshikai, N. Cobalt-Catalyzed Addition of Azoles to Alkynes. *Org. Lett.* **2010**, *12*, 4180-4183. (b) Ding, Z.; Yoshikai, N. Cobalt-Catalyzed Alkenylation of Thiazoles with Alkynes Via C–H Bond Functionalization. *Synthesis* **2011**, 2561-2566.

(21) (a) Gao, K.; Yoshikai, N. Low-Valent Cobalt Catalysis: New Opportunities for C-H Functionalization. *Acc. Chem. Res.* **2014**, *47*, 1208-1219. (b) Moselage, M.; Li, J.; Ackermann, L. Cobalt-Catalyzed C-H Activation. *ACS Catal.* **2016**, *6*, 498-525.

(22) (a) Wu, C.; Yoshikai, N. Cobalt-Catalyzed Intramolecular Reactions between a Vinylcyclopropane and an Alkyne: Switchable

[5+2] Cycloaddition and Homo-Ene Pathways. *Angew. Chem. Int. Ed.* **2018**, *57*, 6558-6562. (b) Ding, W.; Yoshikai, N. Cobalt-Catalyzed Intermolecular [2+2] Cycloaddition between Alkynes and Allenes. *Angew. Chem. Int. Ed.* **2019**, *58*, 2500-2504. (c) Yang, J.; Yoshikai, N. Cobalt-Catalyzed Annulation of Salicylaldehydes and Alkynes to Form Chromones and 4-Chromanones. *Angew. Chem. Int. Ed.* **2016**, *55*, 2870-2874. (d) Yang, J.; Shen, Y.; Lim, Y. J.; Yoshikai, N. Divergent Ring-Opening Coupling between Cyclopropanols and Alkynes under Cobalt Catalysis. *Chem. Sci.* **2018**, *9*, 6928-6934.

(23) This observation was made during our exploration of cobalt-catalyzed [2 + 2 + 2] cycloaddition between benzonitrile and diphenylacetylene in DMF as the solvent (see below).

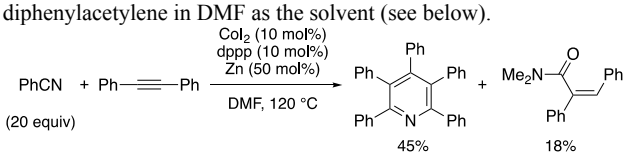

(24) For examples of cobalt/Lewis acid cooperative catalysis, see: (a) Tokmic, K.; Jackson, B. J.; Salazar, A.; Woods, T. J.; Fout, A. R. Cobalt-Catalyzed and Lewis Acid-Assisted Nitrile Hydrogenation to Primary Amines: A Combined Effort. *J. Am. Chem. Soc.* **2017**, *139*, 13554-13561. (b) Kim, J. H.; Greßies, S.; Glorius, F. Cooperative Lewis Acid/Cp*Co^{III} Catalyzed C–H Bond Activation for the Synthesis of Isoquinolin-3-ones. *Angew. Chem. Int. Ed.* **2016**, *55*, 5577-5581.

(25) (a) Guihaumé, J.; Halbert, S.; Eisenstein, O.; Perutz, R. N. Hydrofluoroarylation of Alkynes with Ni Catalysts. C−H Activation Via Ligand-to-Ligand Hydrogen Transfer, an Alternative to Oxidative Addition. *Organometallics* **2012**, *31*, 1300-1314. (b) Bair, J. S.; Schramm, Y.; Sergeev, A. G.; Clot, E.; Eisenstein, O.; Hartwig, J. F. Linear-Selective Hydroarylation of Unactivated Terminal and Internal Olefins with Trifluoromethyl-Substituted Arenes. *J. Am. Chem. Soc.* **2014**, *136*, 13098-13101. (c) Fallon, B. J.; Derat, E.; Amatore, M.; Aubert, C.; Chemla, F.; Ferreira, F.; Perez-Luna, A.; Petit, M. C-H Activation/Functionalization Catalyzed by Simple, Well-Defined Low-Valent Cobalt Complexes. *J. Am. Chem. Soc.* **2015**, *137*, 2448-2451. (d) Xiao, L.-J.; Fu, X.-N.; Zhou, M.-J.; Xie, J.-H.; Wang, L.-X.; Xu, X.-F.; Zhou, Q.-L. Nickel-Catalyzed Hydroacylation of Styrenes with Simple Aldehydes: Reaction Development and Mechanistic Insights. *J. Am. Chem. Soc.* **2016**, *138*, 2957-2960. (e) Eisenstein, O.; Milani, J.; Perutz, R. N. Selectivity of C-H Activation and Competition between C-H and C-F Bond Activation at Fluorocarbons. *Chem. Rev.* **2017**, *117*, 8710-8753. (f) Tang, S.; Eisenstein, O.; Nakao, Y.; Sakaki, S. Aromatic C−H σ-Bond Activation by Ni^0, Pd^0, and Pt^0 Alkene Complexes: Concerted Oxidative Addition to Metal vs Ligand-to-Ligand H Transfer Mechanism. *Organometallics* **2017**, *36*, 2761-2771.

(26) (a) Gao, K.; Lee, P. S.; Fujita, T.; Yoshikai, N. Cobalt-Catalyzed Hydroarylation of Alkynes through Chelation-Assisted C-H Bond Activation. *J. Am. Chem. Soc.* **2010**, *132*, 12249-12251. (b) Gao, K.; Yoshikai, N. Regioselectivity-Switchable Hydroarylation of Styrenes. *J. Am. Chem. Soc.* **2011**, *133*, 400-402. (c) Lee, P. S.; Fujita, T.; Yoshikai, N. Cobalt-Catalyzed, Room-Temperature Addition of Aromatic Imines to Alkynes Via Directed C-H Bond Activation. *J. Am. Chem. Soc.* **2011**, *133*, 17283-17295. (d) Xu, W.; Yoshikai, N. Highly Linear Selective Cobalt-Catalyzed Addition of Aryl Imines to Styrenes: Reversing Intrinsic Regioselectivity by Ligand Elaboration. *Angew. Chem. Int. Ed.* **2014**, *53*, 14166-14170. (e) Xu, W.; Yoshikai, N. N-H Imine as a Powerful Directing Group for Cobalt-Catalyzed Olefin Hydroarylation. *Angew. Chem. Int. Ed.* **2016**, *55*, 12731-12735.

(27) (a) Yang, J.; Yoshikai, N. Cobalt-Catalyzed Enantioselective Intramolecular Hydroacylation of Ketones and Olefins. *J. Am. Chem. Soc.* **2014**, *136*, 16748-16751. (b) Yang, J.; Rerat, A.; Lim, Y. J.; Gosmini, C.; Yoshikai, N. Cobalt-Catalyzed Enantio- and Diastereoselective Intramolecular Hydroacylation of Trisubstituted Alkenes. *Angew. Chem., Int. Ed.* **2017**, *56*, 2449-2453.

(28) (a) Röse, P.; Hilt, G. Cobalt-Catalysed Bond Formation Reactions; Part 2. *Synthesis* **2016**, *48*, 463-492. (b) Gandeepan, P.; Cheng, C.-H. Cobalt Catalysis Involving π Components in Organic Synthesis. *Acc. Chem. Res.* **2015**, *48*, 1194-1206. (c) Hess, W.; Treutwein, J.; Hilt, G. Cobalt-Catalysed Carbon-Carbon Bond-Formation Reactions. *Synthesis* **2008**, 3537-3562.

(29) (a) Treutwein, J.; Hilt, G. Cobalt-Catalyzed [2+2] Cycloaddition. *Angew. Chem. Int. Ed.* **2008**, *47*, 6811-6813. (b) Hilt, G.; Smolko, K. I. Alkynylboronic Esters as Efficient Dienophiles in Cobalt-Catalyzed Diels-Alder Reactions. *Angew. Chem. Int. Ed.* **2003**, *42*, 2795-2797. (c) Nishimura, A.; Tamai, E.; Ohashi, M.; Ogoshi, S. Synthesis of Cyclobutenes and Allenes by Cobalt-Catalyzed Cross-Dimerization of Simple Alkenes with 1,3-Enynes. *Chem. Eur. J.* **2014**, *20*, 6613-6617. (d) Chang, H. T.; Jeganmohan, M.; Cheng, C. H. Cobalt-Catalyzed Intramolecular [2 + 2 + 2] Cocyclotrimerization of Nitrilediynes: An Efficient Route to Tetra- and Pentacyclic Pyridine Derivatives. *Org. Lett.* **2007**, *9*, 505-508. (e) Achard, M.; Tenaglia, A.; Buono, G. First Cobalt(I)-Catalyzed [6 + 2] Cycloadditions of Cycloheptatriene with Alkynes. *Org. Lett.* **2005**, *7*, 2353-2356.

(30) Fujihara, T.; Katafuchi, Y.; Iwai, T.; Terao, J.; Tsuji, Y. Palladium-Catalyzed Intermolecular Addition of Formamides to Alkynes. *J. Am. Chem. Soc.* **2010**, *132*, 2094-2098.

(31) (a) Koubachi, J.; Kazzouli, S. E.; Bousmina, M.; Guillaumet, G. Functionalization of Imidazo[1,2-*a*]pyridines by Means of Metal-Catalyzed Cross-Coupling Reactions. *Eur. J. Org. Chem.* **2014**, 5119-5138. (b) Bagdi, A. K.; Hajra, A. Design, Synthesis, and Functionalization of Imidazoheterocycles. *Chem Rec.* **2016**, *16*, 1868-1885. (c) Ravi, C.; Adimurthy, S. Synthesis of Imidazo[1,2-a]pyridines: C-H Functionalization in the Direction of C-S Bond Formation. *Chem Rec.* **2017**, *17*, 1019-1038. (d) Yu, Y.; Su, Z.; Cao, H. Strategies for Synthesis of Imidazo[1,2-*a*]pyridine Derivatives: Carbene Transformations or C–H Functionalizations. *Chem Rec.* **2019**, *19*, 2105-2118.

(32) Samanta, S.; Hajra, A. Mn(II)-Catalyzed C−H Alkylation of Imidazopyridines and N-Heteroarenes via Decarbonylative and Cross-Dehydrogenative Coupling. *J. Org. Chem.* **2019**, *84*, 4363-4371.

(33) CCDC 1979149 contains the supplementary crystallographic data for this paper. These data can be obtained free of charge from The Cambridge Crystallographic Data Centre.

(34) (a) Lautens, M.; Tam, W.; Lautens, J. C.; Edwards, L. G.; Crudden, C. M.; Smith, A. C. Cobalt-Catalyzed [2π + 2π + 2π (Homo Diels-Alder) [2π + 2π + 4π] Cycloadditions of Bicyclo[2.2.1]Hepta-2,5-Dienes. *J. Am. Chem. Soc.* **1995**, *117*, 6863-6879. (b) Pagar, V. V.; RajanBabu, T. V. Tandem Catalysis for Asymmetric Coupling of Ethylene and Enynes to Functionalized Cyclobutanes. *Science* **2018**, *361*, 68-72.

(35) (a) Friedfeld, M. R.; Zhong, H.; Ruck, R. T.; Shevlin, M.; Chirik, P. J. Cobalt-Catalyzed Asymmetric Hydrogenation of Enamides Enabled by Single-Electron Reduction. *Science* **2018**, *360*, 888-893. (b) Zhong, H.; Friedfeld, M. R.; Chirik, P. J. Syntheses and Catalytic Hydrogenation Performance of Cationic Bis(Phosphine) Cobalt(I) Diene and Arene Compounds. *Angew. Chem. Int. Ed.* **2019**, *58*, 9194-9198.

(36) All the DFT calculations were performed using Gaussian 09 program package. See the Supporting Information for the detail of the computational methods.

(37) Zell, D.; Bursch, M.; Müller, V.; Grimme, S.; Ackermann, L. Full Selectivity Control in Cobalt(III)-Catalyzed C–H Alkylations by Switching of the C–H Activation Mechanism. *Angew. Chem. Int. Ed.* **2017**, *56*, 10378-10382.

(38) (a) Mayer, I. Charge, Bond Order and Valence in the *ab initio* SCF Theory. *Chem. Phys. Lett*, **1983**, *97*, 270-274. (b) Mayer, I. Improved Definition of Bond Orders for Correlated Wave Functions. *Chem. Phys. Lett.* **2012**. *544*, 83-86.

(39) The Mayer bond orders and ADCH atomic charges were calculated using Multiwfn 3.7. see: Lu, T.; Chen, F. A Multifunctional Wavefunction Analyzer. *J. Comput. Chem.* **2012**, *33*, 580-592.

(40) Lu, T.; Chen, F. Atomic Dipole Moment Corrected Hirshfeld Population Method. *J. Theor. Comput. Chem.* **2012**, 11, 163-183.

(41) Bickelhaupt, F. M.; Houk, K. N. Analyzing Reaction Rates

with the Distortion/Interaction-Activation Strain Model. *Angew. Chem. Int. Ed.* **2017**, *56*, 10070-10086.

(42) Gandeepan, P.; Muller, T.; Zell, D.; Cera, G.; Warratz, S.; Ackermann, L. 3d Transition Metals for C-H Activation. *Chem. Rev.* **2019**, *119*, 2192-2452.